Article

Not peer-reviewed version

Experimental Investigation and Mechanism Analysis of Direct Aqueous Mineral Carbonation Using Steel Slag

Fuxia Zhu , Longpeng Cui , Yanfang Liu , Liang Zou , Jili Hou , Chenghao Li , Ge Wu , Run Xu , Bo Jiang * , Zhiqiang Wang *

Posted Date: 31 October 2023

doi: 10.20944/preprints202310.2023.v1

Keywords: Steel slag; Direct aqueous carbonation; CO2 sequestration; Parameter optimization; Mechanism analysis

Article

Experimental Investigation and Mechanism Analysis of Direct Aqueous Mineral Carbonation Using Steel Slag

Fuxia Zhu [1], Longpeng Cui [1], Yanfang Liu [1], Liang Zou [1], Jili Hou [1], Chenghao Li [1], Ge Wu [1], Run Xu [1], Bo Jiang [2,*] and Zhiqiang Wang [1,*]

[1] Department of Coal and Syngas Conversion, Sinopec Research Institute of Petroleum Processing CO., Ltd., Beijing 100083, China

[2] Department of Environmental Science and Engineering, University of Science and Technology Beijing, Beijing 100083, China

* Correspondence: jiangbo_seee@ustb.edu.cn (B.J.); wangzhiqiang.ripp@sinopec.com (Z.W.); Tel.: +86 010-62332867 (B.J.); +86 010-82368211 (Z.W.)

Abstract: The carbonation of industrial calcium-rich byproducts such as steel slag demonstrates significant potential for CO_2 sequestration. This technique aids in reducing carbon emissions while also promoting waste recycling. Despite its advantages, gaps remain in understanding how steel slag characteristics and operational parameters influence the carbonation process, as well as the underlying mechanism of direct aqueous carbonation. We evaluated the carbonation performance of three types of steel slag at temperatures below 100°C using a gas–liquid–solid reaction system. The slag with the highest CO_2 sequestration capacity was chosen for a systematic evaluation of the effects of operating conditions on carbonation efficiency. Thermodynamic analysis indicated that the reactivity of CaO and $Ca(OH)_2$ with CO_2 exceeded that of $CaO{\cdot}SiO_2$ and $2CaO{\cdot}SiO_2$. Under conditions of 85°C, a particle size less than 75 μm, an initial CO_2 pressure of 0.5 MPa, a liquid-to-solid ratio of 5 mL/g, and a stirring speed of 200 rpm, the steel slag achieved a sequestration capacity (K) of 283.5 gCO_2/kg and a carbonation efficiency (ζ_{Ca}) of 51.61%. Characterization of the slag before and after carbonation using X-ray diffraction, SEM–EDS, thermogravimetric analysis, and Fourier transform infrared spectrometry confirmed the formation of new carbonates. Mechanistic analysis revealed that the rate-limiting step initially involved the mass transfer of CO_2, transitioning to Ca^{2+} mass transfer as time progressed. Our research provides a viable technique for CO_2 capture and a beneficial approach for reutilizing waste steel slag. Furthermore, solid residues after capturing CO_2 have the potential for conversion into carbon-negative building materials, offering a sustainable strategy for steel companies and other enterprises with high carbon emissions.

Keywords: steel slag; direct aqueous carbonation; CO_2 sequestration; parameter optimization; mechanism analysis

1. Introduction

Since the onset of the Industrial Revolution, human production activities have predominantly relied on fossil fuels for energy provision. The combustion of these fossil fuels results in the significant generation of carbon dioxide (CO_2), which plays a notable role in amplifying the greenhouse effect[1,2]. This acceleration of the greenhouse effect has garnered substantial attention from governments worldwide due to its adverse effects on the ecological environment, making the reduction of CO_2 emissions a pressing global concern. According to statistics, China is responsible for as much as 50% of global carbon emissions, solidifying its position as the top emitter in the world[3]. As the largest developing nation globally, China's rapid industrialization has led to an increasing consumption of fossil fuels. While clean energy sources such as solar, wind, and hydrogen are not yet feasible alternatives, fossil fuels continue to predominate[4]. Given this critical situation, China's implementation of a "dual carbon" strategy holds significant importance, and there is an urgent need for the development and research of technologies aimed at reducing CO_2 emissions.

 doi:10.20944/preprints202310.2023.v1

The steel industry is a sector characterized by high energy consumption, accounting for approximately 15% of China's total carbon emissions and standing as one of the primary sources of CO_2. During the steel-making process, solid waste, referred to as steel slag, is produced at a rate of 10–15% of the steel output. As of 2021, global crude steel production has reached 1.951 billion tons, with China's share constituting more than 50% of the global total since 2017, showing a continuous upward trajectory[5,6]. Despite the substantial volume of steel slag generated in China, its effective utilization rate remains below 30%, which is significantly lower than that in developed nations. This excessive accumulation of steel slag not only leads to resource waste but also results in land occupation and environmental degradation[7]. Research has demonstrated that steel slag possesses promising capabilities for the capture and storage of CO_2. Through the mineral carbonation of steel slag, it is possible to enhance the material's properties by reducing its content of free calcium oxide (f-CaO) and free magnesium oxide (f-MgO) while simultaneously reducing CO_2 emissions to mitigate the greenhouse effect[8]. Furthermore, CO_2-captured steel slag can be transformed into carbon-negative building materials, thus promoting sustainable development within the steel industry and other high-carbon-emitting sectors.

Mineral carbonation of steel slag for CO_2 sequestration is considered one of the most promising green technologies for achieving the strategic objectives of industrial "dual carbon." Mineral carbonation processes can be categorized into indirect and direct carbonation. Indirect carbonation entails the extraction of Ca/Mg from steel slag using a leaching agent, followed by solid–liquid separation to obtain a solution rich in calcium and magnesium ions, which subsequently undergo carbonation reactions with CO_2 to produce $CaCO_3$ and $MgCO_3$[9]. Although this method can yield high-purity carbonate products, it is plagued by extended leaching reaction times, complex process flows, and substantial energy consumption for leaching agent regeneration and recycling, all of which hinder its large-scale industrial application.

Direct carbonation can be further classified into dry and methods. In the dry method, a gas–solid phase reaction occurs, wherein CO_2 gas diffuses into the steel slag and reacts with its active components. However, the dense structure of steel slag impedes CO_2 diffusion, resulting in sluggish carbonation rates, even under elevated temperatures and initial CO_2 pressure conditions. These low conversion rates render it unsuitable for industrial-scale applications[10,11]. Santos et al.[12] investigated the dry method carbonation of steel slag and found that under conditions of a reaction temperature T=500°C, CO_2 concentration of 75%, initial CO_2 pressure P_{CO_2} =3 bar, and reaction time t=50 min, the sequestration capacity and carbonation efficiency were 83.8 gCO_2/kg and 29%, respectively. Ghouleh et al.[13] determined that reaction time and temperature are the primary factors influencing the carbonation conversion of steelmaking slags. At 650°C and an initial CO_2 pressure of 20 bar, they achieved a maximum carbonization conversion of 26%, equivalent to a capacity of 120 gCO_2/kg.

In the wet method, a gas–liquid-solid three-phase system is present; CO_2 dissolves in water to form carbonic acid, and steel slag gradually dissolves in a weakly acidic solution, subsequently precipitating as carbonates upon reacting with bicarbonate ions[14]. This method demonstrates favorable kinetic properties under lower temperatures and initial CO_2 pressures, necessitating reduced energy input, thereby augmenting its economic feasibility. The majority of studies involving steel slag for CO_2 mineralization primarily focus on the wet method of direct carbonation. Ibrahim et al.[15] employed response surface methodology to investigate the effects of initial CO_2 pressure on the aqueous carbonation reactions of steel slag. The results indicate that within a specific range, decreasing the solid-to-liquid ratio and increasing the pressure can enhance CO_2 sequestration. Under conditions of T=25°C, 100% vol. CO_2, P_{CO_2} =1 bar, and L/S=20 mL/g, the CO_2 sequestration capacity reached 283 gCO_2/kg, accompanied by a carbonation efficiency of 67%. Chang et al.[16] utilized a rotating packed bed to examine the aqueous carbonation of steel slag, revealing that the most influential operational parameter affecting carbonation kinetics was the reaction temperature. Under optimal conditions of 65°C, 750 rpm, and t=30 min, a CO_2 sequestration capacity of 404.8 gCO_2/kg and a carbonation efficiency of up to 93.5% were achieved. Furthermore, He et al.[17] employed machine learning to model and predict the CO_2 sequestration process using steel slag

 doi:10.20944/preprints202310.2023.v1

slurry, investigating the effect of process parameters and slag composition on CO_2 sequestration. However, current research primarily centers on the effects of particle size, temperature, reaction time, CO_2 concentration, and pressure on carbonation performance, while the underlying mechanism of carbonation remains incompletely understood and necessitates further investigation.

Building upon the aforementioned analysis, this study initiates an exploration into the carbonation performance of various types of steel slag at low temperatures (<100°C). Through the characterization of samples before and after carbonation, the reaction mechanism of steel slag carbonation is elucidated, and from a thermodynamic standpoint, the reactivity of diverse calcium-based components in steel slag toward CO_2 is analyzed. Subsequently, the study explores the effects of particle size, temperature, initial CO_2 pressure, liquid-to-solid ratio, and stirring speed on the carbonation performance of steel slag. A comprehensive investigation into the mass transfer mechanism of CO_2 capture within a gas–liquid-solid three-phase system employing steel slag is also undertaken. This research makes a valuable contribution to the reduction of carbon emissions and enhancement of the resource recycling rate of steel slag, thereby facilitating the development of a circular economy.

2. Materials and Methods

2.1. Materials

The steel slag samples utilized in this investigation were sourced from three steel mills situated in Shandong Province, China, and were designated SS-1, SS-2, and SS-3. These samples underwent an initial drying process at 105°C until a constant weight was achieved, followed by sieving to obtain samples of varying particle sizes: >180 μm, 180~150 μm, 150~120 μm, 120~75 μm, and <75 μm. Table 1 presents the chemical composition of the steel slag samples. The pure CO_2 employed for the experiments was procured from Beijing Huanyu Jinghui Gas Technology Co., Ltd., with a volume fraction of 99.9%.

Table 1. Chemical composition of different steel slag samples.

Sample	wt(%)									
	SiO_2	Al_2O_3	Fe_2O_3	CaO	MgO	TiO_2	Na_2O	K_2O	P_2O_5	SO_3
SS-1	22.21	1.35	0.39	64.73	6.25	1.07	0.02	0.00	0.00	0.23
SS-2	9.47	1.98	24.44	51.79	5.95	0.71	0.08	0.05	1.45	0.41
SS-3	16.80	4.42	24.90	39.10	4.38	1.00	0.338	0.40	1.47	1.32

2.2. Experimental Section

Figure 1 illustrates a schematic diagram of the experimental setup. In each carbonation experiment, a specific quantity of deionized water and sample were introduced into a high-pressure autoclave reactor and heated to the desired temperature. Subsequently, CO_2 was introduced into the reactor until the preset pressure was attained, and mechanical stirring commenced with precise timing. Following a reaction period of 2 h, the heating process was terminated, and the reactor was rapidly cooled to room temperature. The suspension within the reactor was subsequently subjected to filtration using 0.7 μm filter paper, and the solid fraction was subjected to drying at 105°C for a duration of 24 h. The carbonation performance of the steel slag was quantified through thermogravimetric analysis (TG) conducted on the dried solids.

Preprints (www.preprints.org) | NOT PEER-REVIEWED | Posted: 31 October 2023 doi:10.20944/preprints202310.2023.v1

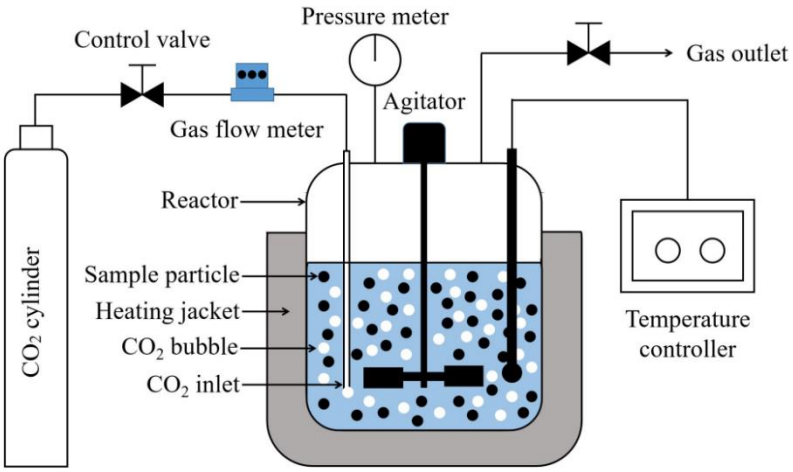

Figure 1. Schematic of the experimental apparatus.

On the one hand, the study involved a comparison of the carbonation performance of three distinct types of steel slag under the following conditions: a temperature of 65°C; an initial CO_2 pressure of 2.0 MPa; a liquid-to-solid ratio of 15 mL/g; a stirring speed of 200 rpm; and a particle size of <75 μm. On the other hand, the investigation explored the effects of various parameters, including particle size (>180 μm, 180~150 μm, 150~120 μm, 120~75 μm, <75 μm), reaction temperature (25°C, 45°C, 65°C, 85°C, and 105°C), initial CO_2 pressure (0.1, 0.5, 1.0, 1.5, and 2.0 MPa), liquid-to-solid ratio (1, 5, 10, 15, 20 mL/g), and stirring speed (200, 400, 600, 800 rpm), on the carbonation performance of steel slag.

2.3. Calculation of Carbonation Performance

TG analysis is performed using a thermogravimetric analyzer to quantify the weight loss experienced by steel slag at elevated temperatures, allowing for the precise determination of the quantity of CO_2 sequestered by the steel slag. The method entails placing a defined mass of the carbonated steel slag product into the thermogravimetric analyzer and subjecting the sample to heating, with a temperature range spanning from 50°C to 950°C, at a rate of 10°C per minute while maintaining an N_2 atmosphere. The temperature was held constant at 105°C and 550°C for a duration of 10 min each, followed by a 5-min dwell at 950°C. Weight losses observed within the temperature ranges of 50°C-105°C, 105°C-550°C, and 550°C-950°C correspond to water evaporation, the decomposition of $Ca(OH)_2$ and $MgCO_3$, and the decomposition of $CaCO_3$, respectively. The quantity of CO_2 is computed based on the dry weight of the carbonated sample and its weight loss within the 550°C-950°C range, following Eq. (1):

$$\omega_{CO_2}[\mathrm{wt\%}]=\frac{\Delta m_{550\text{-}950℃}[\mathrm{g}]}{m_{105℃}[\mathrm{g}]}\times 100\% \quad (1)$$

Sequestration capacity (K) and carbonation efficiency (ζ_{Ca}) are used to evaluate the extent of the carbonation reaction, calculated according to Eqs. (2) and (3):

$$K[\mathrm{gCO_2/kg}]=\frac{\omega_{CO_2}[\mathrm{wt\%}]}{1-\omega_{CO_2}[\mathrm{wt\%}]}\times 1000 \quad (2)$$

Preprints (www.preprints.org) | NOT PEER-REVIEWED | Posted: 31 October 2023 doi:10.20944/preprints202310.2023.v1

$$\zeta_{Ca}[\%]=\frac{\frac{\omega_{CO_2}[wt\%]}{1-\omega_{CO_2}[wt\%]}\times\frac{M_{Ca}[g/mol]}{M_{CO_2}[g/mol]}}{Ca_{total}[wt\%]} \quad (3)$$

where M_{Ca} and M_{CO_2} represent the molar masses of Ca and CO_2, respectively, while Ca_{total} denotes the Ca content in fresh steel slag samples.

2.4. Sample Characterization

The chemical compositions of the samples were analyzed via X-ray fluorescence spectroscopy. The crystal phases of the samples, both before and after carbonation, were investigated using X-ray diffraction (XRD) with Cu-Ka radiation operating at 40 kV and 40 mA. The 2θ scanning angle range for XRD analysis spanned from 10° to 70°, employing a step size of 0.01°.

To observe the microstructure of the samples and assess the surface elemental distribution, thereby identifying the formation of carbonates, scanning electron microscopy coupled with energy-dispersive spectroscopy (SEM–EDS, SU8100) was employed. Fourier transform infrared spectroscopy (FTIR) was utilized for the analysis of the principal chemical bonds present in the samples both before and after the carbonation reaction. Furthermore, changes in the specific surface area and pore size distribution of the steel slag samples, both before and after the carbonation, were examined via Brunauer Emmett Teller (BET) analysis. Finally, the particle size distribution of the samples was determined using a laser particle size analyzer.

3. Results and Discussion

3.1. Carbonation Performance of Different Steel Slags

Table 2 displays the carbonation performance of the three distinct types of steel slag under identical experimental conditions. The sequestration capacities (K) for steel slag samples SS-1, SS-2, and SS-3 were determined to be 106.8, 191.9, and 136.9 gCO_2/kg, respectively. The ability of industrial solid waste to sequester CO_2 is not solely contingent on the content of alkaline components but also influenced by its phase composition[18]. Steel slag primarily comprises four calcium-based active components: CaO, $Ca(OH)_2$, $CaO{\cdot}SiO_2$, and $2CaO{\cdot}SiO_2$. The reaction equations involving these four components in the carbonation process, along with their corresponding Gibbs free energy changes ($\Delta_r G_m^{\theta}$, kJ/mol), are presented in Table 3[19–21]. At a temperature of 65°C, the Gibbs free energy changes for the reactions between these calcium-based active components and CO_2 are as follows: -124.22, -69.19, -38.67, and -57.17 kJ/mol. This indicates that all reactions proceed spontaneously, with the reactivity ranking as follows: CaO > $Ca(OH)_2$ > $2CaO{\cdot}SiO_2$> $CaO{\cdot}SiO_2$.

Figure 2 illustrates the XRD spectra of the three types of steel slag. It is evident that the phase composition of SS-2 and SS-3 substantially differs from that of SS-1. In SS-2 and SS-3, the primary calcium-based active component is $Ca(OH)_2$, while in SS-1, it also includes $CaO{\cdot}SiO_2$ and $2CaO{\cdot}SiO_2$. Thermodynamic analysis reveals that $Ca(OH)_2$ exhibits higher reactivity with CO_2 compared to $CaO{\cdot}SiO_2$ or $2CaO{\cdot}SiO_2$, which elucidates the superior carbonation performance of SS-2 and SS-3 relative to SS-1. Additionally, as indicated in Table 1, SS-2 boasts higher contents of CaO and MgO, at 51.76% and 5.95%, respectively, in contrast to 39.10% and 4.38% in SS-3. Consequently, the carbonation performance of SS-2 surpasses that of SS-3. Subsequent investigations will focus on SS-2 to explore the influence of particle size (d), temperature (T), pressure (p), liquid-to-solid ratio (L/S), and rotational speed (r) on the carbonation performance of steel slag.

Table 2. Carbonation performance of different steel slag samples (operating parameters: 65°C, 2 MPa initial CO_2 pressure, 15 mL/g liquid-to-solid ratio, 200 rpm stirring speed).

Sample	K (gCO_2/kg)
SS-1	106.8
SS-2	191.9

Preprints (www.preprints.org) | NOT PEER-REVIEWED | Posted: 31 October 2023 doi:10.20944/preprints202310.2023.v1

SS-3	136.9

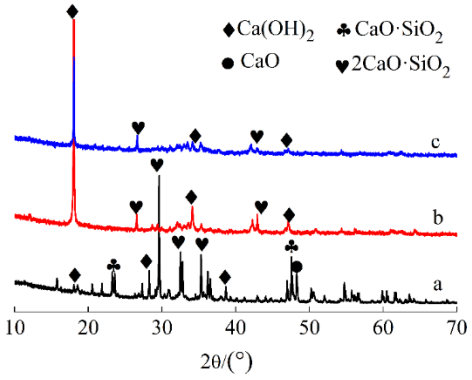

Figure 2. XRD spectra of different steel slag samples, (a) SS-1; (b) SS-2; (c) SS-3.

Table 3. Potential carbon sequestration reactions of the main calcium-based active components in steel slag and their Gibbs free energies at 65°C (atmospheric pressure).

Phase	Reaction equation	$\Delta_r G_m^\theta$[kJ /mol]
		65°C
CaO	$CaO+CO_2 \rightarrow CaCO_3$	-124.22
$Ca(OH)_2$	$Ca(OH)_2+H_2O+CO_2 \rightarrow CaCO_3+2H_2O$	-69.19
$CaO·SiO_2$	$CaO·SiO_2+H_2O+CO_2 \rightarrow CaCO_3+SiO_2·H_2O$	-38.67
$2CaO·SiO_2$	$(2CaO·SiO_2)+H_2O+2CO_2 \rightarrow 2CaCO_3+SiO_2·H_2O$	-57.17

3.2. Sample Characterization

3.2.1. TG Analysis

Figure 3 illustrates the weight loss curves for SS-2 steel slag both before and after the carbonation reaction. The unprocessed sample exhibits a noticeable weight loss within the temperature range of 105–550°C, which corresponds to the decomposition of $Ca(OH)_2$, indicating the presence of $Ca(OH)_2$ in the original sample. After undergoing the carbonation reaction, the weight loss in the 105–550°C range notably diminishes, whereas the weight loss between 550–950°C experiences a significant increase, reaching 21.92%. This observation implies that following the carbonation reaction, $Ca(OH)_2$ reacts with CO_2 to yield $CaCO_3$.

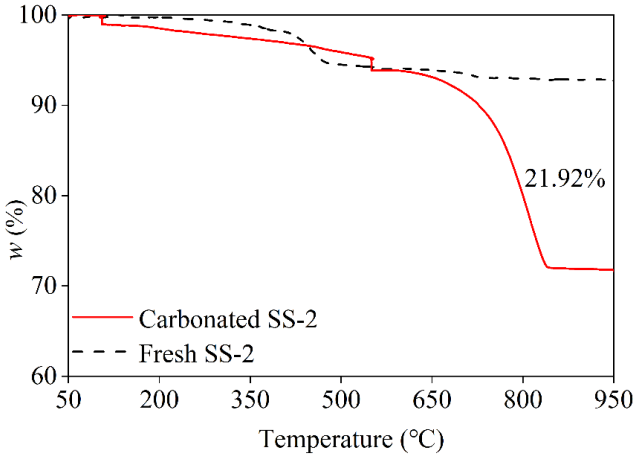

Figure 3. Thermal gravimetrical curves of fresh and carbonated SS-2 samples.

Preprints (www.preprints.org) | NOT PEER-REVIEWED | Posted: 31 October 2023 doi:10.20944/preprints202310.2023.v1

3.2.2. XRD Analysis

Figure 4 presents the XRD spectra of SS-2 steel slag both before and after the carbonation reaction. The initial SS-2 steel slag primarily contains $Ca(OH)_2$ and $2CaO{\cdot}SiO_2$. However, following carbonation, the peak corresponding to $Ca(OH)_2$ vanishes, the peak for $2CaO{\cdot}SiO_2$ weakens, and the $CaCO_3$ peak intensifies. These findings affirm that $Ca(OH)_2$ in the initial SS-2 steel slag undergoes complete conversion into $CaCO_3$ through carbonation, a conclusion supported by the results of TG analysis of the carbonated slag. Additionally, the partial carbonation of $2CaO{\cdot}SiO_2$ into $CaCO_3$ suggests that $Ca(OH)_2$ displays a greater reactivity with CO_2 compared to $2CaO{\cdot}SiO_2$, aligning with the thermodynamic analysis (Table 3).

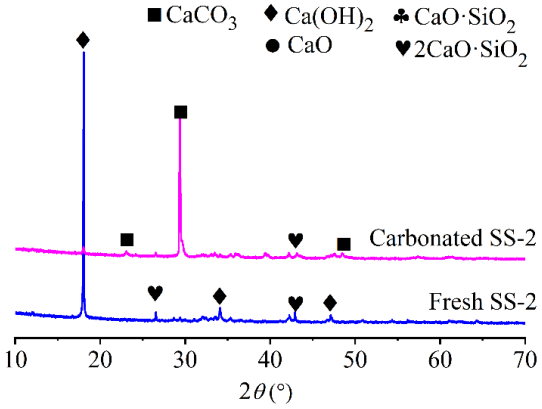

Figure 4. XRD patterns of fresh and carbonated SS-2 samples.

3.2.3. SEM–EDS analysis

Figure 5a,b provide an illustration of the crystal morphology of SS-2 steel slag both before and after the carbonation reaction. The morphology of the initial SS-2 steel slag is characterized by particle aggregation with unevenly distributed pores. Notable morphological transformations occur subsequent to carbonation, including the emergence of numerous cubic particle crystals that aggregate. Complementing after the carbonation energy-dispersive spectroscopy (EDS) analysis (Fig. 5c), the composition is unequivocally identified as $CaCO_3$, a finding that corroborates the results of XRD phase analysis. However, it is important to note that the surface development of $CaCO_3$ appears uneven following the carbonation reaction. This nonuniformity may impede the penetration of unreacted slag into the liquid phase, thereby increasing the difficulty of further reactions between the unreacted Ca-based active phases within the slag and CO_2. Consequently, this could limit the slag's CO_2 sequestration capacity[8]. Furthermore, freshly carbonated slag comprises particles of varying sizes, exhibiting a surface rich in fine-pore structures. In contrast, carbonated samples form dense aggregates with a relatively uniform particle size.

Preprints (www.preprints.org) | NOT PEER-REVIEWED | Posted: 31 October 2023 doi:10.20944/preprints202310.2023.v1

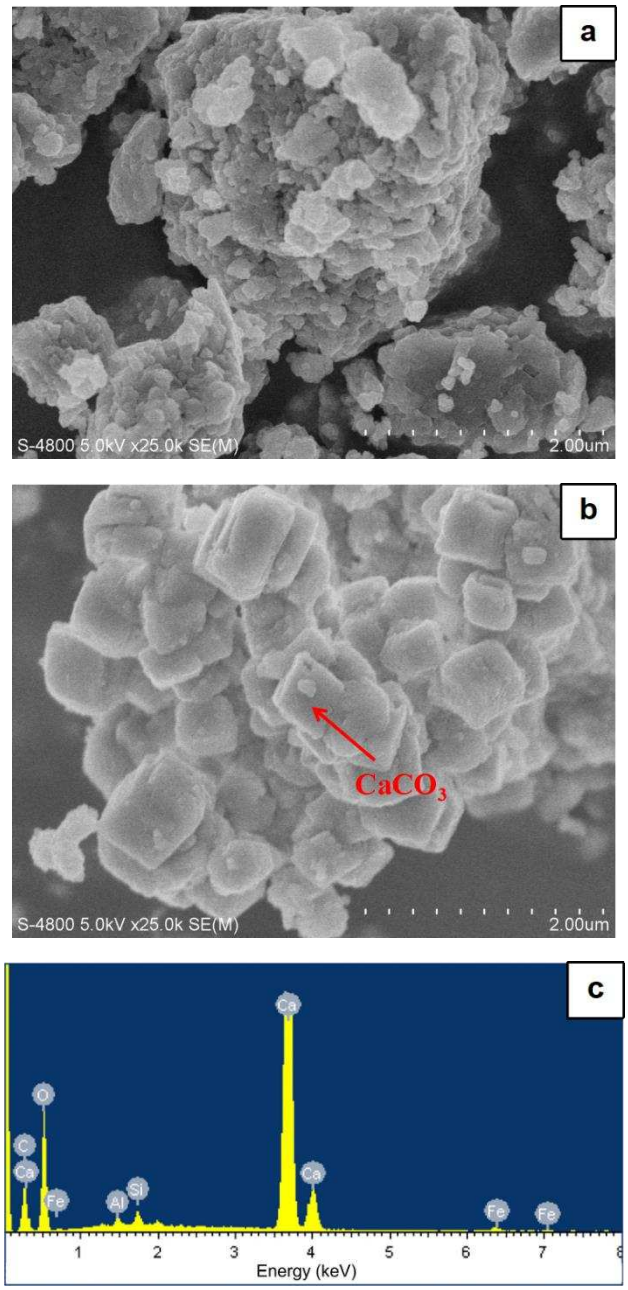

Figure 5. SEM–EDS images of (a) fresh and (b) carbonated steel slags.

3.2.4. FTIR Spectra

Figure 6 presents the infrared spectra of SS-2 steel slag both before and after the carbonation reaction. The spectrum of the initial SS-2 steel slag not only reveals a broad absorption peak at 3422 cm^{-1} but also displays a narrower peak at 3644 cm^{-1}. This narrower peak at 3644 cm^{-1} corresponds to the H-O stretching vibrations in $Ca(OH)_2$[22], thus confirming the presence of $Ca(OH)_2$. This observation aligns with the previous XRD phase analysis and TG results. Subsequent to the carbonation reaction of SS-2 steel slag, prominent absorption peaks emerge in the resulting material at 715 cm^{-1}, 880 cm^{-1}, and 1450 cm^{-1}. Specifically, the peak at 715 cm^{-1} corresponds to the in-plane bending vibration of the O-C-O group in $CaCO_3$; the peak at 880 cm^{-1} represents the out-of-plane bending vibration of the O-C-O group; and the peak at 1450 cm^{-1} is associated with the C-O antisymmetric stretching vibrations in $CaCO_3$[23]. These distinctive features provide compelling evidence that the primary product of the carbonation reaction is indeed $CaCO_3$.

Preprints (www.preprints.org) | NOT PEER-REVIEWED | Posted: 31 October 2023 doi:10.20944/preprints202310.2023.v1

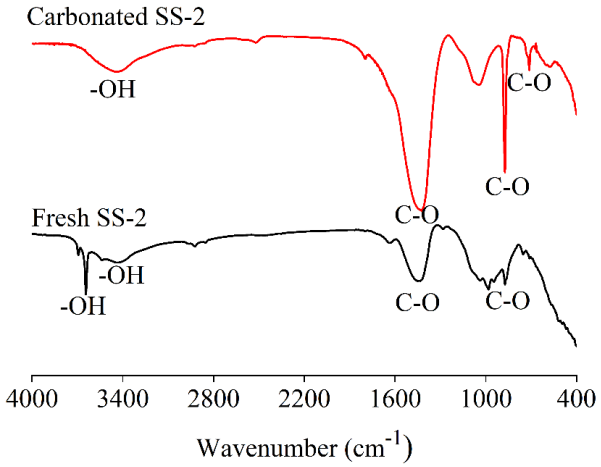

Figure 6. FTIR spectra of fresh and carbonated SS-2 samples.

3.3. Effect of Operating Parameters on the Carbonation of Steel Slag

3.3.1. Effect of Particle Size

Figure 7 depicts the effect of particle size on direct aqueous carbonation under constant temperature (65°C), initial CO_2 pressure (2 MPa), liquid-to-solid ratio (15 mL/g), and stirring speed (200 rpm) conditions. It is evident that as the particle size decreases below 180 μm, both the sequestration rate (*K*) and the carbonation rate ζ_{Ca} exhibit a notable increase. Specifically, *K* rises from 50.8 gCO_2/kg to 219.5 gCO_2/kg, and ζ_{Ca} increases from 10.20% to 40.27%. This observed increase can be attributed to the growth in the specific surface area of the steel slag as the particle size diminishes (as detailed in Table 4). Simultaneously, the milled steel slag undergoes a reduction in lattice energy, leading to the generation of lattice dislocations, defects, and recrystallization at sites where lattice energy is lost. These alterations facilitate an expanded contact area between the slag minerals and CO_2, thereby enhancing the interaction forces between the minerals and CO_2 and accelerating the carbonation reaction[24]. Consequently, the optimal particle size for the direct aqueous carbonation of steel slag is less than 75 μm.

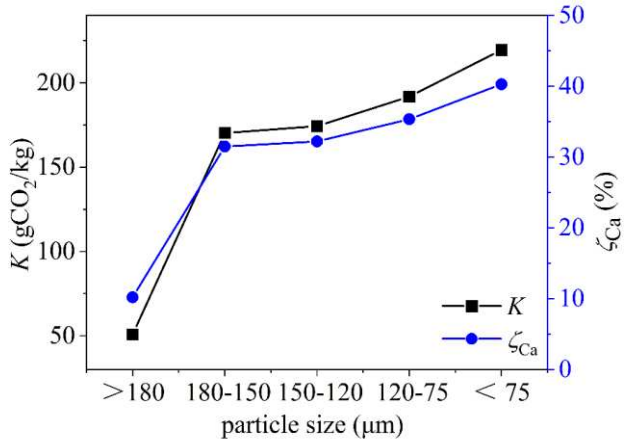

Figure 7. Influence of particle size on the carbonation performance of steel slag.

Table 4. BET analysis of SS-2 particles of different sizes.

Sample Parameter	unit	>180	180~150	150~120	120~75	<75

Preprints (www.preprints.org) | NOT PEER-REVIEWED | Posted: 31 October 2023 doi:10.20944/preprints202310.2023.v1

BET surface area	m^2/g	2.0045	10.2273	10.9660	13.9087	14.1616
Total pore volume	cm^3/g	0.005434	0.021842	0.023745	0.029356	0.037526

3.3.2. Effect of Reaction Temperature

Figure 8 illustrates the effect of reaction temperature on the direct aqueous carbonation of steel slag, considering particle sizes smaller than 200 μm, an initial CO_2 pressure of 2 MPa, a liquid-to-solid ratio of 15 mL/g, and a stirring speed of 200 rpm. This observation indicates that the carbonation performance of steel slag experiences a decline as the temperature varies from 25°C to 45°C. However, a significant enhancement in carbonation performance is noted as the temperature rises from 45°C to 85°C, with the sequestration capacity (*K*) increasing from 157.9 gCO_2/kg to 260.7 gCO_2/kg and the carbonation rate ζ_{Ca} increasing from 29.29% to 47.62%. Beyond this temperature range, only marginal increases in both *K* and ζ_{Ca} are noted.

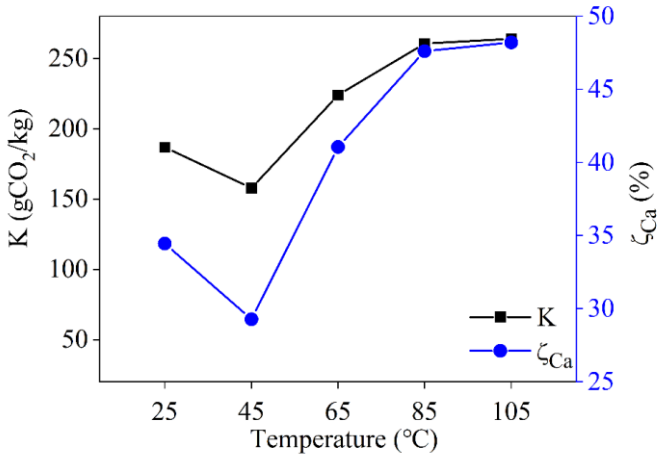

Figure 8. Influence of reaction temperature on the carbonation performance of steel slag.

This finding contrasts with our prior research on the effect of temperature on the carbonation performance of carbide slag [18]. The disparity can be attributed to the distinct phase compositions of carbide slag and steel slag. Carbide slag primarily comprises $Ca(OH)_2$, which readily dissociates into Ca^{2+} ions at lower temperatures for reaction with CO_2. Below 65°C, the leaching of Ca^{2+} ions constitutes the rate-limiting step in the reaction. With a further temperature increase, the solubility of CO_2 rapidly diminishes, hindering the formation of CO_3^{2-} ions and subsequently the precipitation of $CaCO_3$, making CO_2 dissolution the new rate-limiting step [15].

In contrast, steel slag possesses a more complex phase composition, including both $Ca(OH)_2$ and $2CaO{\cdot}SiO_2$. The Ca^{2+} ions in $2CaO{\cdot}SiO_2$ are more challenging to dissociate, necessitating higher temperatures for effective leaching. Therefore, below 45°C, CO_2 dissolution serves as the rate-limiting step. As the temperature increases, Ca^{2+} leaching becomes the rate-limiting step for carbonation. The leaching rate of Ca^{2+} accelerates, and the amount leached increases within a certain time frame, thus promoting $CaCO_3$ formation [25]. Consequently, the optimal temperature for the direct aqueous carbonation of steel slag is found to be 85°C.

3.3.3. Effect of Initial CO_2 Pressure

Figure 9 illustrates the effect of the initial CO_2 pressure on the direct aqueous carbonation of steel slag, maintaining a reaction temperature of 105°C, a particle size smaller than 200 μm, a liquid-to-solid ratio of 15 mL/g, and a stirring speed of 200 rpm. As observed, when the pressure is below 0.5 MPa, both the sequestration capacity (*K*) and the carbonation rate ζ_{Ca} increase significantly with rising pressure. The *K* value escalates from 166.9 gCO_2/kg to 214.8 gCO_2/kg, while the carbonation rate ζ_{Ca} improves from 30.88% to 39.42%. However, beyond the threshold of 0.5 MPa, a plateau is

Preprints (www.preprints.org) | NOT PEER-REVIEWED | Posted: 31 October 2023 doi:10.20944/preprints202310.2023.v1

reached in both *K* and ζ_{Ca} upon increasing the pressure to 2.0 MPa. Consequently, the optimal initial CO_2 pressure for the direct aqueous carbonation of steel slag is determined to be 0.5 MPa.

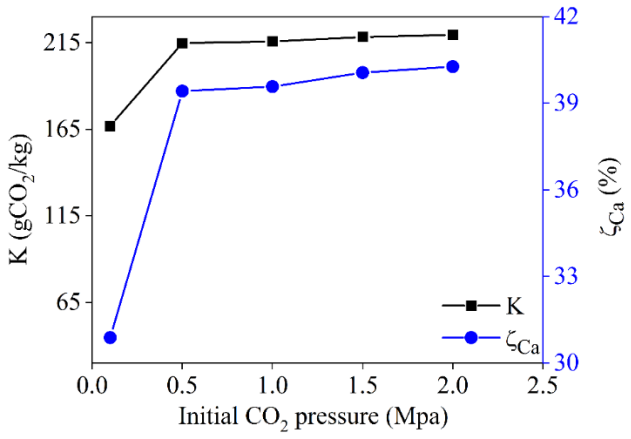

Figure 9. Influence of initial CO_2 pressure on the carbonation performance of steel slag.

$$[CO_2] = k_{co_2} \times P(CO_2) \quad (4)$$

The influence of the initial CO_2 pressure on the CO_2 sequestration capacity of steel slag can be explained through Henry's Law (Eq. 4). In Eq. 5, $[CO_2]$ represents the concentration of CO_2 in water, while k_{CO_2} is Henry's constant and $P(CO_2)$ is the partial pressure of CO_2 gas. At a constant temperature, the solubility of CO_2 molecules is directly proportional to pressure, indicating that a higher initial CO_2 pressure leads to increased dissolution of CO_2 in the slurry. This enhanced dissolution facilitates the formation of $CaCO_3$ precipitates.

For steel slag, when $P(CO_2) < 0.5$ MPa, the dissolution of CO_2 serves as the rate-limiting step, and both the sequestration capacity (*K*) and the carbonation rate ζ_{Ca} primarily depend on the concentration of CO_3^{2-} ions. As the initial CO_2 pressure increases, the concentration of CO_2, and consequently, the generated CO_3^{2-} ions in the slurry rise, resulting in an increase in both *K* and ζ_{Ca}. When $P(CO_2) > 0.5$ MPa, the leaching of Ca^{2+} ions from the solid matrix becomes the rate-limiting step. At this juncture, the CO_2 concentration in the slurry has already reached saturation and no longer influences the carbonation efficiency. Instead, the intrinsic properties of the raw material govern the carbonation performance [26].

3.3.4. Effect of the Liquid-to-Solid Ratio

Figure 10 depicts the effect of the liquid-to-solid ratio on the direct aqueous carbonation of steel slag under specific conditions: a constant reaction temperature of 105°C, a particle size less than 200 μm, an initial CO_2 pressure of 0.5 MPa, and a stirring speed of 200 rpm. It is evident that when the liquid-to-solid ratio is less than 5 mL/g, both the sequestration capacity (*K*) and the carbonation rate ζ_{Ca} increase significantly. Specifically, *K* escalates from 98.2 gCO_2/kg to 217.6 gCO_2/kg, while the carbonation rate ζ_{Ca} rises from 10.73% to 39.92%. However, with further increases in the liquid-to-solid ratio, there is a decline in both *K* and ζ_{Ca}. The optimal liquid-to-solid ratio for the direct aqueous carbonation of steel slag is identified as 5 mL/g.

Preprints (www.preprints.org) | NOT PEER-REVIEWED | Posted: 31 October 2023 doi:10.20944/preprints202310.2023.v1

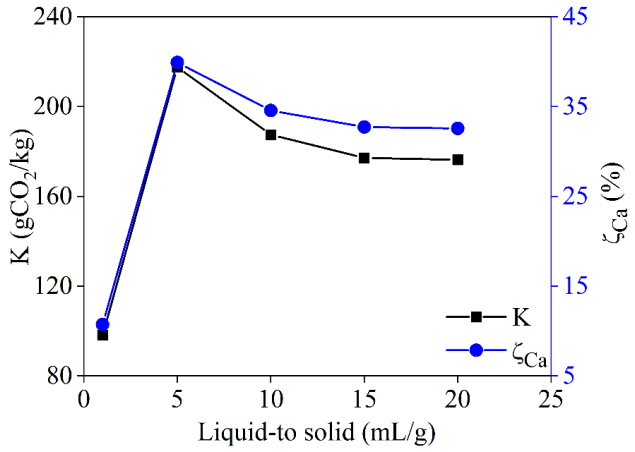

Figure 10. Influence of the liquid-to-solid ratio on the carbonation performance of steel slag.

The direct aqueous carbonation process of steel slag is closely linked to the diffusion and dissolution of CO_2 in water, as well as the dissolution of alkaline substances in steel slag. Prior to reaching a liquid-to-solid ratio of 5 mL/g, water acts as the medium that facilitates the reaction between the solid matrix and gaseous CO_2. However, the leaching of Ca^{2+} ions from the solid matrix is insufficient, limiting the extent of the reaction. As the liquid-to-solid ratio continues to increase, excess water in the reaction system impedes the permeation of CO_2 due to capillary forces. This hindrance inhibits the contact between CO_2 and active reaction sites, resulting in incomplete carbonation. Consequently, the carbonation efficiency of steel slag decreases [27].

3.3.5. Effect of Stirring Speed

Figure 11a displays the influence of rotational speed on the direct aqueous carbonation of steel slag under the following conditions: a reaction temperature of 105°C, particle size less than 200 μm, initial CO_2 pressure of 0.5 MPa, and liquid-to-solid ratio of 15 mL/g. As the rotational speed increases from 200 rpm to 800 rpm, both the sequestration capacity K and the carbonation rate ζ_{Ca} experience a minor increase, indicating that rotational speed has a marginal effect on the carbonation performance of steel slag. However, as shown in Figure 11b, elevating the rotational speed enhances the reaction rate of the direct aqueous carbonation of steel slag. This enhancement may be attributed to an increased contact area or a thinner diffusion layer, facilitating better interaction among the gas, liquid, and solid phases[28]. Additionally, higher stirring rates might induce erosive effects on the particles, improving the reactivity of the solid matrix surface and preventing the newly formed $CaCO_3$ precipitate from coating unreacted sample surfaces[29].

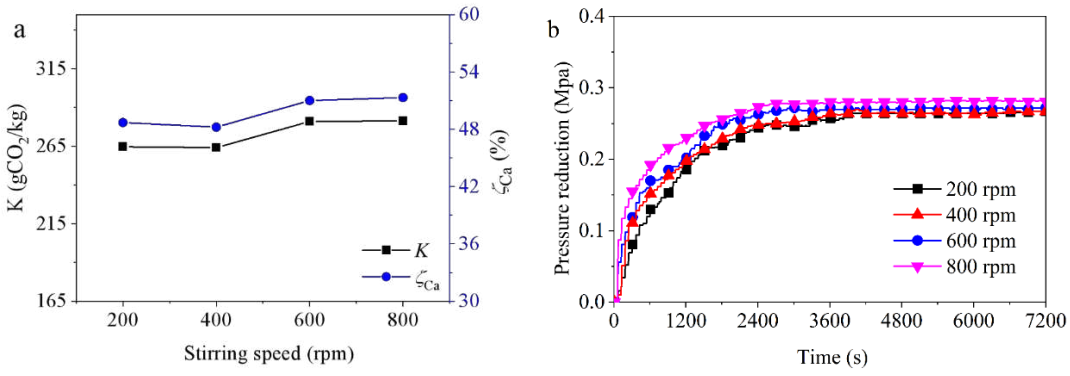

Figure 11. Influence of stirring speed on the carbonation performance of steel slag and (b) carbonation pressure reduction of steel slag with time for different stirring speeds.

Preprints (www.preprints.org) | NOT PEER-REVIEWED | Posted: 31 October 2023 doi:10.20944/preprints202310.2023.v1

3.4. Mechanism Analysis of Steel Slag for CO_2 Sequestration

The chemical reactions involved in the direct aqueous carbonation of steel slag include [30]:

I. Dissolution of CO_2 in the liquid phase to form H_2CO_3 ($H_2CO_3(H_2O+CO_2 \rightarrow H_2CO_3)$;

II. Dissociation of H_2CO_3 to form HCO_3^- or CO_3^{2-} ions $(H_2CO_3 \rightarrow HCO_3^- + H^+; HCO_3^- \rightarrow CO_3^{2-} + H^+)$;

III. Irreversible hydration of CaO in steel slag $(CaO + H_2O \rightarrow Ca(OH)_2)$, dissolution and ionization of $Ca(OH)_2 (Ca(OH)_2 \rightarrow Ca^{2+} + 2OH^-)$;

IV. Reaction between CO_3^{2-} and Ca^{2+} ions to form $CaCO_3 (Ca^{2+} + CO_3^{2-} \rightarrow CaCO_3)$.

The process of direct aqueous carbonation of steel slag occurs in two stages, as depicted in Figure 12. In the first stage, CO_2 molecules diffuse from the gas phase into the gas film and then to the gas–liquid interface, ultimately dissolving into the liquid phase. This diffusion process follows the dual-film theory. The active components in steel slag diffuse from the solid interior to the liquid film at the solid–liquid interface, a process described by Fick's law. Carbonation between CO_3^{2-} and Ca^{2+} ions initiates in the liquid film near the gas–liquid interface, where unreacted calcium-based active components in steel slag particles gradually shrink[31]. The formed $CaCO_3$ is primarily in the liquid phase, with a minor fraction coating unreacted steel slag particles. The diffusion rate of Ca^{2+} ions is relatively higher than that of CO_2, keeping the concentration of Ca^{2+} ions constant in the liquid phase. Therefore, mass transfer of CO_2 between the gas and liquid phases controls the rate of the carbonation reaction.

In the second stage, CO_2 molecules diffuse from the liquid film to the liquid film at the solid–liquid interface, and the carbonation reaction between Ca^{2+} and CO_3^{2-} ions also shifts to this film. Simultaneously, unreacted components in steel slag particles continue to shrink. The diffusion rate of Ca^{2+} ions decreases, resulting in a lower concentration of Ca^{2+} ions in the liquid phase. The formed calcium carbonate primarily coats the steel slag particle surfaces, impeding further dissolution of Ca^{2+} ions and reducing the rate of the carbonation reaction. Consequently, mass transfer of Ca^{2+} ions between the solid and liquid phases controls the reaction rate [32].

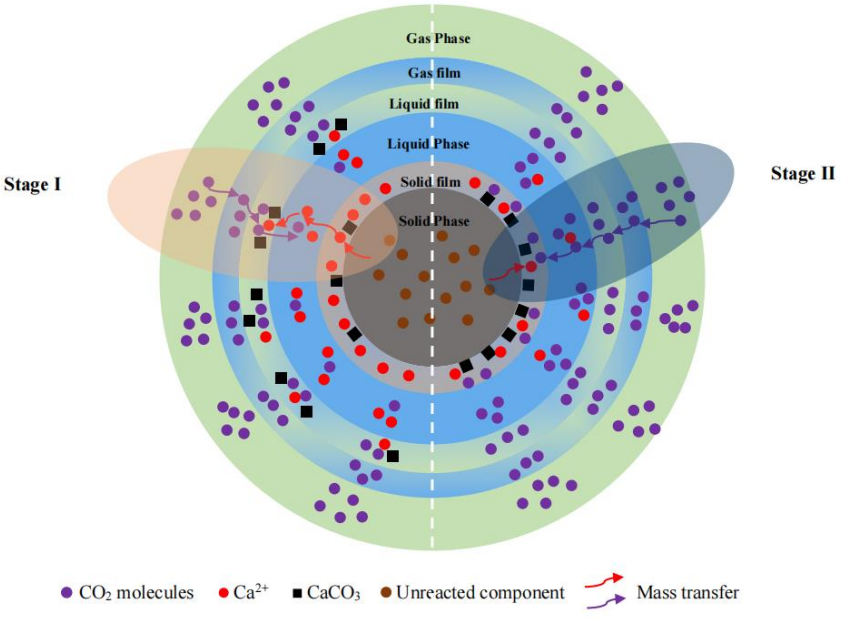

Figure 12. Mechanism analysis of direct aqueous mineral carbonation of steel slag.

4. Conclusions

(1) Particle size, temperature, pressure, and liquid-to-solid ratio significantly influence both the sequestration rate *K* and carbonation rate ζ_{Ca} of steel slag, while the effect of stirring speed is minor. The optimal carbonation performance of steel slag is observed under the following conditions: particle size < 75 μm, reaction temperature at 105°C, initial CO_2 pressure of 0.5 MPa, and liquid-to-solid ratio of 5 mL/g. Under these conditions, the sequestration and carbonation rates reached 283 gCO_2/kg and 51.61%, respectively.

(2) Various characterization techniques, including XRD, SEM–EDS, TG, and FTIR, were employed to analyze steel slag samples before and after carbonation, confirming the formation of calcium carbonate. From a thermodynamic perspective, the sequence of reactivity among the four calcium-based active components in steel slag with CO_2 is as follows: CaO $Ca(OH)_2$ > >$2CaO{\cdot}SiO_2$ > $CaO{\cdot}SiO_2$.

(3) The direct aqueous carbonation process of steel slag can be divided into two stages: in the initial stage, the rate-limiting step is the mass transfer of CO_2; as time progresses, the mass transfer of Ca^{2+} becomes the controlling factor for the carbonation rate.

References

1. Rahmanihanzaki, M.; Hemmati, A., A review of mineral carbonation by alkaline solidwaste. *International Journal of Greenhouse Gas Control* **2022,** 121, 103798.
2. Kamkeng, A. D. N.; Wang, M.; Hu, J.; Du, W.; Qian, F., Transformation technologies for CO2 utilisation: Current status, challenges and future prospects. *Chemical Engineering Journal* **2021,** 409, 128138.
3. Pan, S.-Y.; Chen, Y.-H.; Fan, L.-S.; Kim, H.; Gao, X.; Ling, T.-C.; Chiang, P.-C.; Pei, S.-L.; Gu, G., CO2 mineralization and utilization by alkaline solid wastes for potential carbon reduction. *Nature Sustainability* **2020,** 3, (5), 399-405.
4. Lei, L.; Bai, L.; Lindbråthen, A.; Pan, F.; Zhang, X.; He, X., Carbon membranes for CO2 removal: Status and perspectives from materials to processes. *Chemical Engineering Journal* **2020,** 401, 126084.
5. Ferrara, G.; Belli, A.; Keulen, A.; Tulliani, J.-M.; Palmero, P., Testing procedures for CO2 uptake assessment of accelerated carbonation products: Experimental application on basic oxygen furnace steel slag samples. *Construction and Building Materials* **2023,** 406, 133384.
6. Dziejarski, B.; Krzyżyńska, R.; Andersson, K., Current status of carbon capture, utilization, and storage technologies in the global economy: A survey of technical assessment. *Fuel* **2023,** 342, 127776.
7. Liu, J.; Zeng, C.; Li, Z.; Liu, G.; Zhang, W.; Xie, G.; Xing, F., Carbonation of steel slag at low CO2 concentrations: Novel biochar cold-bonded steel slag artificial aggregates. *Science of The Total Environment* **2023,** 902, 166065.
8. Zhang, Y.; Yu, L.; Cui, K.; Wang, H.; Fu, T., Carbon capture and storage technology by steel-making slags: Recent progress and future challenges. *Chemical Engineering Journal* **2023,** 455, 140552.
9. Loria, P.; Bright, M. B. H., Lessons captured from 50 years of CCS projects. *The Electricity Journal* **2021,** 34, (7), 106998.
10. Cheng, C.; Huang, W.; Xu, H.; Liu, Z.; Li, X.; Shi, H.; Yu, Y.; Qu, Z.; Yan, N., CO2 sequestration and CaCO3 recovery with steel slag by a novel two-step leaching and carbonation method. *Science of The Total Environment* **2023,** 891, 164203.
11. Fu, L.; Ren, Z.; Si, W.; Ma, Q.; Huang, W.; Liao, K.; Huang, Z.; Wang, Y.; Li, J.; Xu, P., Research progress on CO2 capture and utilization technology. *Journal of CO2 Utilization* **2022,** 66.
12. Santos, R. M.; Ling, D.; Sarvaramini, A.; Guo, M.; Elsen, J.; Larachi, F.; Beaudoin, G.; Blanpain, B.; Van Gerven, T., Stabilization of basic oxygen furnace slag by hot-stage carbonation treatment. *Chemical Engineering Journal* **2012,** 203, 239-250.
13. Ghouleh, Z.; Guthrie, R. I. L.; Shao, Y., High-strength KOBM steel slag binder activated by carbonation. *Construction and Building Materials* **2015,** 99, 175-183.
14. Li, Z.; Chen, J.; Lv, Z.; Tong, Y.; Ran, J.; Qin, C., Evaluation on direct aqueous carbonation of industrial/mining solid wastes for CO2 mineralization. *Journal of Industrial and Engineering Chemistry* **2023,** 122, 359-365.
15. Ibrahim, M. H.; El-Naas, M. H.; Zevenhoven, R.; Al-Sobhi, S. A., Enhanced CO2 capture through reaction with steel-making dust in high salinity water. *International Journal of Greenhouse Gas Control* **2019,** 91, 102819.
16. Chang, E. E.; Pan, S.-Y.; Chen, Y.-H.; Tan, C.-S.; Chiang, P.-C., Accelerated carbonation of steelmaking slags in a high-gravity rotating packed bed. *Journal of Hazardous Materials* **2012,** 227-228, 97-106.
17. He, B.; Zhu, X.; Cang, Z.; Liu, Y.; Lei, Y.; Chen, Z.; Wang, Y.; Zheng, Y.; Cang, D.; Zhang, L., Interpretation and Prediction of the CO2 Sequestration of Steel Slag by Machine Learning. *Environmental Science & Technology* **2023**.

18. Wang, Z.; Cui, L.; Liu, Y.; Hou, J.; Li, H.; Zou, L.; Zhu, F., High-efficiency CO2 sequestration through direct aqueous carbonation of carbide slag: determination of carbonation reaction and optimization of operation parameters. *Frontiers of Environmental Science & Engineering* **2023,** 18, (1), 12.
19. Yadav, S.; Mehra, A., Experimental study of dissolution of minerals and CO2 sequestration in steel slag. *Waste Management* **2017,** 64, 348-357.
20. Pan, S.-Y.; Hung, C.-H.; Chan, Y.-W., Integrated CO2 Fixation, Waste Stabilization, and Product Utilization via High-Gravity Carbonation Process Exemplified by Circular Fluidized Bed Fly Ash. *ACS Sustainable Chemistry & Engineering* **2016,** 4, (6).
21. Huijgen, W. J. J.; Comans, R. N. J., Carbonation of steel slag for CO2 sequestration: leaching of products and reaction mechanisms. *Environmental Science & Technology* **2006,** 40, (8), 2790-2796.
22. Qin, L.; Gao, X., Properties of coal gangue-Portland cement mixture with carbonation. *Fuel* **2019,** 245, 1-12.
23. Yang, C.; Yang, X.; Zhao, T.; Liu, F., An indirect CO2 utilization for the crystallization control of CaCO3 using alkylcarbonate. *Journal of CO2 Utilization* **2021,** 45, 101448.
24. Li, X.; Mehdizadeh, H.; Ling, T.-C., Environmental, economic and engineering performances of aqueous carbonated steel slag powders as alternative material in cement pastes: Influence of particle size. *Science of The Total Environment* **2023,** 903, 166210.
25. Ukwattage, N. L.; Ranjith, P. G.; Yellishetty, M.; Bui, H. H.; Xu, T., A laboratory-scale study of the aqueous mineral carbonation of coal fly ash for CO2 sequestration. *Journal of Cleaner Production* **2015,** 103, 665-674.
26. Omale, S. O.; Choong, T. S. Y.; Abdullah, L. C.; Siajam, S. I.; Yip, M. W., Utilization of Malaysia EAF slags for effective application in direct aqueous sequestration of carbon dioxide under ambient temperature. *Heliyon* **2019,** 5, (10), e02602.
27. Tamilselvi Dananjayan, R. R.; Kandasamy, P.; Andimuthu, R., Direct mineral carbonation of coal fly ash for CO2 sequestration. *Journal of Cleaner Production* **2016,** 112, 4173-4182.
28. Georgakopoulos, E.; Santos, R. M.; Chiang, Y. W.; Manovic, V., Influence of process parameters on carbonation rate and conversion of steelmaking slags – Introduction of the 'carbonation weathering rate'. *Greenhouse Gases: Science and Technology* **2016,** 6, (4), 470-491.
29. N, H. D.; S, G. J.; Komar, K. S.; C, E. T.; L, S. L., Carbon dioxide sequestration in cement kiln dust through mineral carbonation *Environmental science & technology* **2009,** 43, (6).
30. Polettini, A.; Pomi, R.; Stramazzo, A., CO2 sequestration through aqueous accelerated carbonation of BOF slag: A factorial study of parameters effects. *Journal of Environmental Management* **2016,** 167, 185-195.
31. Wang, C.; Xu, Z.; Lai, C.; Sun, X., Beyond the standard two-film theory: Computational fluid dynamics simulations for carbon dioxide capture in a wetted wall column. *Chemical Engineering Science* **2018,** 184, 103-110.
32. Yang, J.; Liu, S.; Ma, L.; Zhao, S.; Liu, H.; Dai, Q.; Yang, Y.; Xu, C.; Xin, X.; Zhang, X.; Liu, J., Mechanism analysis of carbide slag capture of CO2 via a gas-liquid-solid three-phase fluidization system. *Journal of Cleaner Production* **2021,** 279, 123712.